

PAPER • OPEN ACCESS

Determination of the uncertainty of microhardness in the evaluation of hardfacing obtained by welding

To cite this article: A Cruz-Crespo *et al* 2015 *J. Phys.: Conf. Ser.* **648** 012004

View the [article online](#) for updates and enhancements.

You may also like

- [Refinement of \$M_7C_3\$ in hypereutectic Fe-based hardfacing coating and interface behavior of \(Ti, Nb\)\(C,N\)/ \$M_7C_3\$ from first-principles](#)
Jibo Wang, Xiaowen Qi, Xiaolei Xing et al.
- [Effectiveness of metal powder additions for martensitic hardfacing alloy on its wear properties](#)
Buntoeng Srikarun, Hein Zaw Oo and Prapas Muangjunburee
- [Effects of load on abrasive-wear behavior of Nb-strengthening hypoeutectic Fe-Cr-C hardfacing alloy at a 2-body abrasives environment](#)
Mingyang Lian, Runzhen Yu, Zhiquan Huang et al.



ECS
The
Electrochemical
Society
Advancing solid state &
electrochemical science & technology

DISCOVER
how sustainability
intersects with
electrochemistry & solid
state science research

Determination of the uncertainty of microhardness in the evaluation of hardfacing obtained by welding

A Cruz-Crespo¹, J E S Leal², A Piratelli-Filho³, T O Mendez⁴ and R V Arencibia⁵

^{1,4} Central University “Marta Abreu” of Las Villas. Research Center of Welding, Road to Camajuaní, 5 ½ km Santa Clara, Villa Clara, Cuba

^{2,5} Federal University of Uberlândia, 2121, João Naves de Ávila Avenue, Campus Santa Mônica, Building 5F, Zip Code: 38400-902, Uberlândia – MG. Brazil

³ University of Brasília, Faculty of Technology, Department of Mechanical Engineering, University Campus Darcy Ribeiro, Asa Norte, 70910-900, Brasília, DF, Brazil

E-mail: arvaldes@mecanica.ufu.br

Abstract. The present work evaluates the microhardness measurement uncertainty using a Vickers indenter in the characterization of hard deposits, obtained with experimental electrode for hardfacing of cutting knives in sugar mills. The following stages were proposed: i) obtainment of the deposit with experimental electrode, ii) obtainment of the samples, iii) chemical characterization, iv) metallographic analysis, v) microhardness measurement and vi) uncertainty measurement assessment. It was observed that the obtained deposit presents chrome carbides and eutectic matrix composed of austenite and carbides. The expanded uncertainty associated to the microhardness measurement is highly influenced by the low repeatability of the obtained microhardness values.

1. Introduction

The sugar industry is characterized by the presence of various mechanical components subject to abrasive wear and continuous rubbing occur during manufacturing and components recovery. Among these components, the knife is an essential element that affects the milling process efficiency ratios.

Literature [1-2] reported that abrasion, corrosion and impact are wear mechanisms to which are submitted the knives' working edges, with the last one the less likely to occur nowadays due to the care and cleaning treatment of sugar cane prior to reach the feeding table, being the abrasion considered as the main wearing mechanism.

It is common practice the covering of the knives working edges using the Shielded Metal Arc Welding process (SMAW), with abrasion-resistant alloys of the type AWS 5:13 EF and Cr -A1A, which pour a (not diluted) chemical composition in weight (%) varying from 3.5% to 4.5% carbon, 4.0% to 6.0% manganese, 0.5% to 2.0% silicon and 20% to 25% chromium [3-4].

The AWS A5.13 [3] Standard establishes 26 types of surface coating consumables cast iron base (Fe) for SMAW. From these, 22 offer good resistance properties to abrasive wear, seven of which yield an alloying system with proper resistance at low pressure working conditions. The main alloying elements of such consumables are C, Mn, Si, Cr and Mo, with elements Ni (4%) and Ti (1.8%) being introduced separately [3].



The coating of knives and other components subjected to abrasion is carried upon the composition, microstructure and properties of the deposits, and also on technological criteria for applying the coating process. Note that, studies on the use of processing criteria that lead to a reliable interpretation of the results and their metrological traceability are scarce in the literature.

This work aims at determining the aspects that affect the microhardness measurement uncertainty in the characterization of hard coatings obtained with an experimental electrode applied to knives used in the sugar industry.

2. Methodology

The characterization of the deposit with experimental electrode applied to knives used in sugar mills [5] was carried out at the Central University of Welding Research Center Martha Abreu de Las Villas, Cuba. In order to obtain samples for chemical and structural analysis, it was used the standard SFA 5:13 [3] which establishes the size of the deposit (50 mm, 13 mm and 16 mm for electrodes with 4 mm metal core diameter). During the deposition, it was used a MANSFELD welding source with 110 A direct current and inverted polarity (DC+). The deposition was performed in multiple runs by manual welding at an average speed of 15 cm/min at room temperature.

2.1. Chemical analysis

The chemical characterization was made by atomic emission spectroscopy of the sample probes that were extracted through slicing the deposit at the cross section of the top surface.

2.2. Metallographic analysis

For metallographic characterization, the CIS-MET-030 [6] and CIS-MET-027 [7] preparation and samples observation procedures were followed. The samples were taken from the deposit mid portion, cutting them perpendicularly to the welding path. After that, the samples were trimmed, polished, etched with Murakami reagent and finally observed with a NEOPHOT 32 optical metallographic microscope.

2.3. Microhardness measurement

The Vickers microhardness was determined using a Shimatsu microdurometer, as specified by the ASTM E92 [8] Standard. The load applied was 50 gf during 15 s. The imprints were made so that the spacing between them was greater than 0.5 mm, making a total of 15 imprints. The Vickers microhardness was calculated from the diagonal length values (d_1 and d_2) formed by opposite vertices of the pyramid base left by the penetrator. The length of the diagonal was measured by the microscope's micrometer with 400x magnification and resolution 0.25 μm . The expanded uncertainty associated with the calibration is 0.02 μm for a coverage factor (k) equal to 2.00 and 95.45% coverage probability. Each diagonal was measured three times.

The hardness measurement process can be considered a non-destructive test, since the tested part can be reused. However, the damage caused by the indenter in the test point makes impossible to evaluate the process uncertainty by making repeated measurements at the same location [9].

The arithmetic average of the diagonal length values was calculated by equation (1).

$$d = \frac{d_1 + d_2}{2} \quad (1)$$

For each indentation, the Vickers hardness (HV) was determined by equation (2), where F is the load applied during the test and A is the surface area of printing.

$$HV = \frac{F}{A} = \frac{2 \cdot F \cdot \sin \frac{136^\circ}{2}}{d^2} \approx 1.8544 \cdot \frac{F}{d^2} \quad (2)$$

2.4. Uncertainty measurement assessment

The evaluation of measurement uncertainty was performed by applying the methodology proposed by ISO [10]. The main sources of uncertainty in the hardness measurement are related to the sample, hardness testing machine, the environment and the operator [9]. Some works were found on evaluation of microhardness measurement uncertainty. Among them, Ellis [11] considered the following sources of influence related to the testing machine: the linear repeatability, the load, the resolution and the indenter angle.

In this work, it was considered the following influencing factors: the linear repeatability and resolution of the machine, the load, the expansion of the measuring system and the variability of the obtained microhardness, expressed through the sample standard deviation.

Initially, the standard uncertainty associated with the length measurement of the imprint diagonals (d_1 and d_2) were calculated starting from equation (3). In this case, three influence variables were considered to determine the diagonal lengths, d_1 and d_2 .

$$d_1 = d_2 = dm + \Delta R + \Delta IC + \Delta A \quad (3)$$

In this expression: dm represents the measured length of the diagonals d_1 or d_2 ; ΔR is the correction associated to the microscope resolution; ΔIC is the correction associated to the microscope calibration; ΔA is the correction associated to the microscope expansion.

The uncertainty associated with the load applied during the test was declared in the calibration certificate as expanded uncertainty of 0.02 gf with 95.45% coverage probability and coverage factor (k) of 2. The standardization of the expanded uncertainty was performed by means of equation (4).

$$u(F) = \frac{U(F)}{k_F} \quad (4)$$

In this expression: $u(F)$ is the standard uncertainty associated with the applied test load; $U(F)$ is the expanded uncertainty associated with the applied test load and k_F is the coverage factor associated with the expanded uncertainty of the load calibration.

Next, it was determined the standard uncertainty associated with the arithmetical average of the diagonal length values (d), using the mathematical model of equation (1). Finally, the uncertainty associated with the Vickers hardness was determined by means of equation (2).

After applying the uncertainties propagation law in equations (3), (1) and (2), there were obtained the equations (5), (6) and (7), respectively, allowing the estimation of the combined standard uncertainty associated with the measurement of the diagonals' length values, the arithmetic mean of the diagonals' length values and the Vickers hardness.

$$u_c^2(d_1) = \left(\frac{\partial d_1}{\partial dm}\right)^2 \cdot u^2(dm) + \left(\frac{\partial d_1}{\partial \Delta R}\right)^2 \cdot u^2(\Delta R) + \left(\frac{\partial d_1}{\partial \Delta IC}\right)^2 \cdot u^2(\Delta IC) + \left(\frac{\partial d_1}{\partial \Delta A}\right)^2 \cdot u^2(\Delta A) \quad (5)$$

$$u_c^2(d) = \left(\frac{\partial d}{\partial d_1}\right)^2 \cdot u^2(d_1) + \left(\frac{\partial d}{\partial d_2}\right)^2 \cdot u^2(d_2) \quad (6)$$

$$u_c^2(HV) = \left(\frac{\partial HV}{\partial F}\right)^2 \cdot u^2(F) + \left(\frac{\partial HV}{\partial d}\right)^2 \cdot u^2(d) \quad (7)$$

However, several microhardness HV measurements are usually made whose individual uncertainty is determined by means of equation (7), but it was necessary to add a correction to equation (2) as observed in equation (8), where $\Delta s(HV)$ is the correction associated with the microhardness variability. The combined standard uncertainty of these microhardness measurements is finally determined by $u_c(HV)$ in equation (9).

$$HV = \Delta s(HV) + 1.8544 \cdot \frac{F}{d^2} \quad (8)$$

$$u_c^2(HV) = \left(\frac{\partial HV}{\partial \Delta s(HV)} \right)^2 \cdot u^2(\Delta s(HV)) + \left(\frac{\partial HV}{\partial F} \right)^2 \cdot u^2(F) + \left(\frac{\partial HV}{\partial d} \right)^2 \cdot u^2(d) \quad (9)$$

Calculating the partial derivatives in equations (5), (6) and (9), it was obtained the equations (10), (11) and (12), respectively.

$$u_c^2(d_1) = u^2(\Delta R) + u^2(\Delta IC) + u^2(\Delta A) \quad (10)$$

$$u_c^2(d) = \left(\frac{d_2}{2} \right)^2 \cdot u^2(d_1) + \left(\frac{d_1}{2} \right)^2 \cdot u^2(d_2) \quad (11)$$

$$u_c^2(HV) = u^2(\Delta s(HV)) + \left(\frac{1,8544}{d^2} \right)^2 \cdot u^2(F) + \left(\frac{-2 \cdot 1,8544 \cdot F}{d^3} \right)^2 \cdot u^2(d) \quad (12)$$

2.5. Standard uncertainty assessment

The standard uncertainty linked to the microscope resolution was determined by equation (13). Therefore, a Type B assessment was performed, considering a rectangular distribution with infinite degrees of freedom.

$$u(\Delta R) = \frac{\text{Resolution}}{\sqrt{3}} \quad (13)$$

The standard uncertainty linked to the microscope calibration was determined as a Type B evaluation, considering a normal distribution and coverage factor ($k=2$) and the expanded uncertainty stated in the calibration certificate, according to equation (14).

$$u(\Delta IC) = \frac{U(\Delta IC)}{k} \quad (14)$$

The standard uncertainty linked to microscope amplification was calculated by means of a Type B evaluation, considering a rectangular distribution and infinite degrees of freedom. In this case, a distortion was adopted due to the lens magnification corresponding to 0.01% of d_1 and d_2 length values, respectively, as shown in equation (15).

$$u(\Delta A) = \frac{0.01\% \cdot d_1}{\sqrt{3}} \quad (15)$$

The standard uncertainty associated with the variability of the Vickers microhardness ($\Delta s(HV)$) was calculated by means of Type A evaluation, considering a t-Student distribution, and $n-1$ degrees of freedom, where n represents the number of performed indentations or the number of microhardness measurements, equation (16).

$$u(\Delta s(L)) = \frac{s(L)}{\sqrt{n}} \quad (16)$$

3. Results and discussion

The chemical composition of the deposit is shown in table 1. It was observed high content of carbon and chromium, usually characterized by high presence of carbides, being this material suitable for applications in the presence of abrasive wear.

Table 1. Chemical composition of the deposit, in weight %.

Electrode	C	Cr	Mn	Si
Experimental	3.27	15.34	4.09	2.78

Many authors, even when in unbalanced conditions as in the actual solidification process, use the ternary system Fe-Cr-C aiming at generally predicting the phases present in white casting alloys rich in chromium, commonly used in abrasive wear. Among them, Chia-Ming et al. [12] address a study of the microstructure and abrasive wear in coating of hypereutectic alloys with different carbon contents, obtained with self-protecting electrode. Also Hsuan-Han et al. [13] discuss a study of the microstructure of the multilayer coatings of hypoeutectic alloys, obtained via GTAW with transversal oscillation.

Figure 1 shows the liquid projection of the rich in iron vertex of the Fe-Cr-C system, where the point A is situated, corresponding to the deposit of table 1, considering only the elements of the ternary system. It was observed that the point is located in the border of the austenite and M_7C_3 chromium type carbide phases, which also contains iron in the composition $((Cr, Fe)_7C_3)$. The deposit observed microstructure is shown in figure 2.

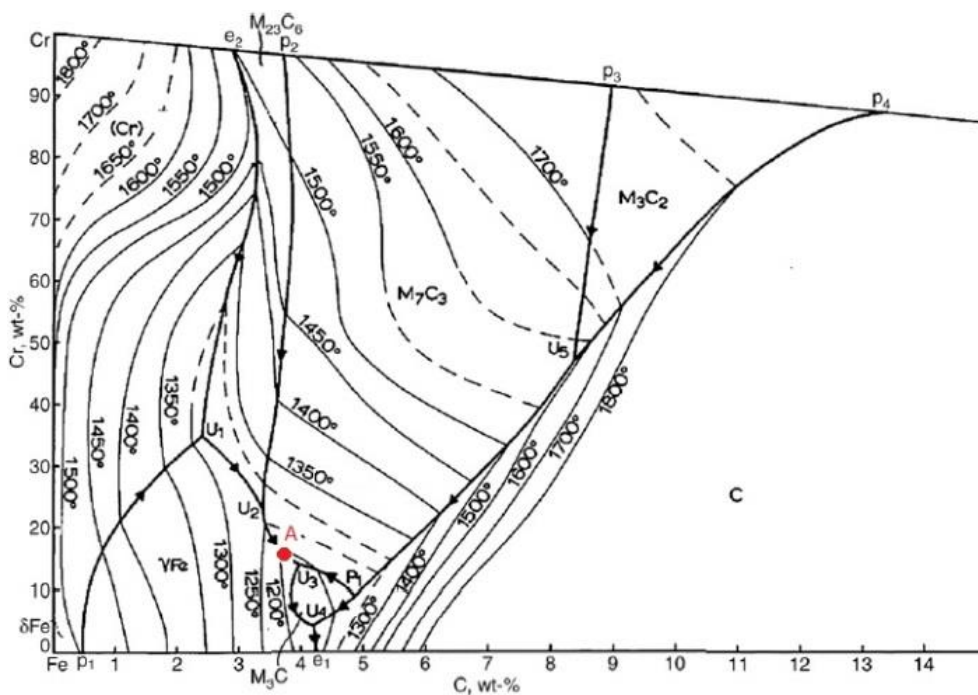


Figure 1. Liquids projection of ternary system Fe-Cr-C to the region rich in iron [12] and [13].

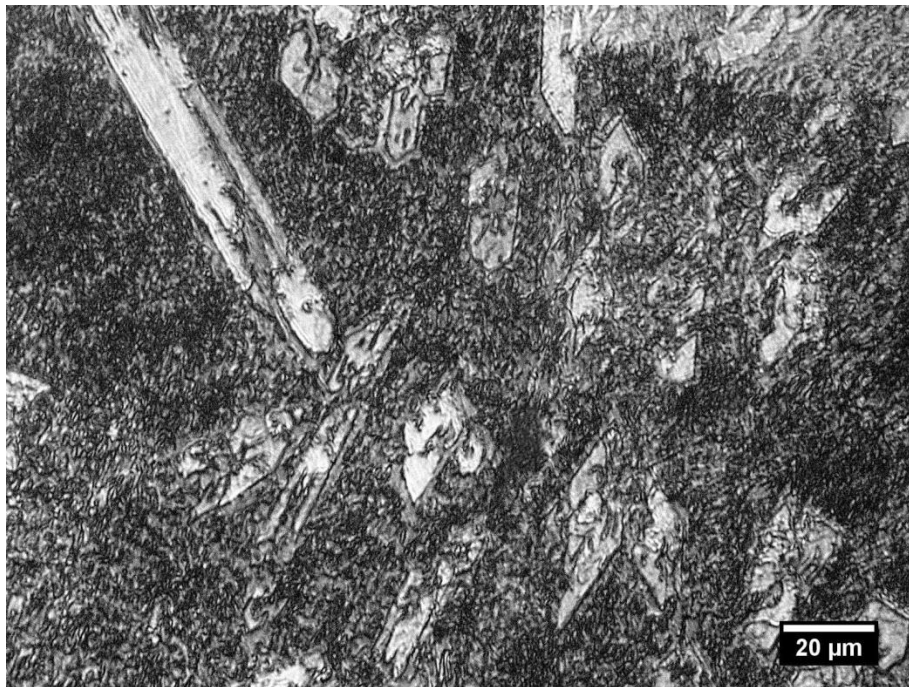


Figure 2. Deposit microstructure.

Figure 2 shows the presence of hexagonal carbides of M_7C_3 type, a noticeably eutectic region (consisting of austenite phases and M_7C_3 carbides) and a clear zone, ascribed to an eutectic region with greater presence of the austenite phase. Thus, the observed microstructure is fully consistent with the analysis of the phases present at the base of the balance ternary system of figure 1.

The presence of primary carbides within an eutectic matrix, which is composed of austenite and small carbides, ensures good resistance to predominating abrasive wear in knives used in sugar mills. In this sense, the result is similar to that reported in the literature for sugar industry applications. For a coating of high-chrome hypereutectic alloy obtained by SMAW, the presence of M_7C_3 type chromium carbides in a eutectic matrix presents characteristics suitable for abrasive wear [14-15].

In figure 3, the average hardness values, with a standard deviation of 68.27% probability, obtained in each zone of the deposit and the corresponding sample standard deviation are shown.

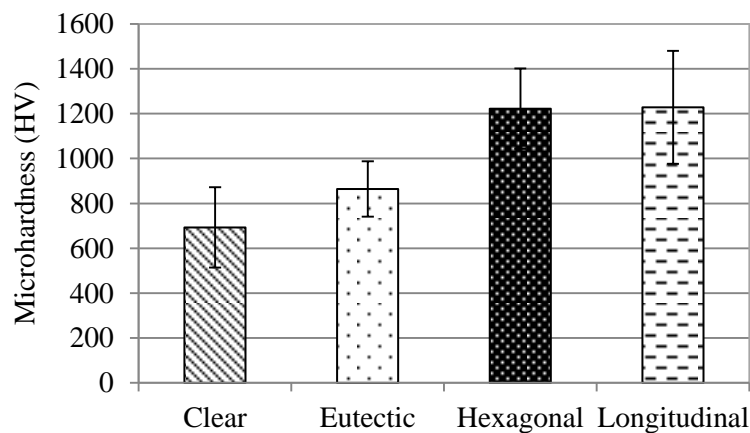


Figure 3. Microhardness mean values of the deposit zones (HV).

Note that in figure 3 the longitudinal cross-section of the deposit's carbides presents the highest microhardness value of 1228 HV , which is relatively similar to the hexagonal section with. On the other hand, the eutectic region exhibits a hardness of 864 HV while the clear zone presents 693 HV .

The average microhardness values coincide with the values commonly reported by several authors, including Chia-Ming et al. [12], who in a study of several coatings with different carbon contents, obtained by welding with tubular electrode, obtained carbides and eutectic microhardness values in a range within which are the values achieved in this study.

It is worthy of note that the identified clear (white) regions also have eutectic matrix, but as they solidify too late get lesser amount of carbides and higher amount of austenite, probably this fact was also influenced by the pro-austenitic effect of manganese present in the deposit (table 1).

With respect to measurement repeatability, it was observed that, for a 68.27% probability, the longitudinal area has a standard deviation of 252 HV , while the eutectic and hexagonal areas exhibit lower values as 179 HV . In the literature are generally referred high microhardness dispersion values of microstructural constituents of white high chrome castings.

For example, Stevenson and Hutchings [16] in a study of the wear behavior of various coatings, show high variability of carbides microhardness values, with standard deviation of 210 HV , while the eutectic matrix displays 125 HV standard deviation.

The footprint of the imprint left by the Vickers indenter is small, allowing the hardness determination of individual micro constituents of a microstructure, however the small size of the imprint contributes to a lower repeatability of the measurement.

The repeatability of the hardness measurement can be significantly influenced by the operator, depending on his training, thoroughness and skill [17]. The operator is the one who determines the boundaries of the diagonal imprints during measurement with microscope. Thus, according to the method used, the parameter "operator skill" has a significant influence on the final result of the measure, and it may represent a major source of error and consequently of uncertainty [18].

Next, the Chauvenet criterion was applied to eliminate extreme values (outliers). In this case were identified only 2 microhardness values that do not follow the mainstream and so were discarded, which are highlighted in table 2 in gray. Again, the arithmetic mean and the standard deviation were calculated.

By eliminating the extreme values, the repeatability of measuring hardness was improved in the clear and the hexagonal zones, showing a reduction of about 48% and 16% , respectively.

It was also observed in table 2 that the microhardness values corresponding to the deposit's clear zone have two perfectly distinguishable populations of values, with much lower values than those expected in the austenite phase; therefore, it can be deduced that there are minute dispersed carbides imperceptible under optical microscopy. In turn, the eutectic zone shows appropriate values for this constituent, in correspondence with the values of the alloying elements.

On the other hand, the microhardness of the carbides shows appropriate values, but it should be noted that their high dispersion may be a possible consequence of heterogeneous crystallization caused by the particular conditions of cooling, characteristic of the welding deposition process and the alloy composition that lead to an extreme imbalance state. The heterogeneity of the carbides microhardness values was associated to the heterogeneity of their own chemical composition as a result of heterogeneous nucleation.

Table 2. Microhardness values of the deposit (HV) after applying Chauvenet criterion.

	Clear	Eutectic	Hexagonal	Longitudinal
1	633	726	1095	897
2	689	766	1049	909
3	700	1006	946	927
4	810	810	1254	965
5	714	857	1197	1027
6	557	841	1283	1095
7	1254	726	1072	1145
8	739	909	1283	1254
9	633	946	1524	1283
10	603	985	1254	1346
11	473	1095	1225	1396
12	753	655	1605	1486
13	689	927	1314	1524
14	540	946	1225	1564
15	603	766	1005	1605
Average	653	864	1195	1228
Standard deviation	92	123	150	252

Figure 4 shows the imprint area values left by the Vickers indenter in the first measurement area in each zone of the evaluated deposit. As expected, a clear zone has the highest area value (0.023 mm^2), while the Longitudinal zone has the lowest value (0.012 mm^2).

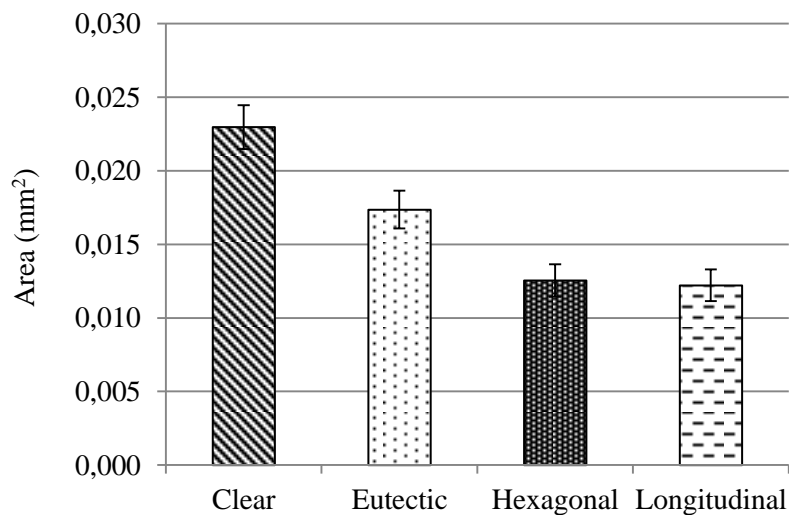


Figure 4. Area values and the associated combined standard uncertainty (68.27%).

With respect to the combined standard uncertainty associated with the area measurement, it was observed that it takes similar values for the four evaluated zones, with 0.0015 mm^2 for the Clear zone, 0.0013 mm^2 for the Eutectic and 0.0011 mm^2 for the Hexagonal and Longitudinal zones.

Figure 5 shows the expanded uncertainty values associated with the microhardness measurement in the four considered zones for 95% coverage probability.

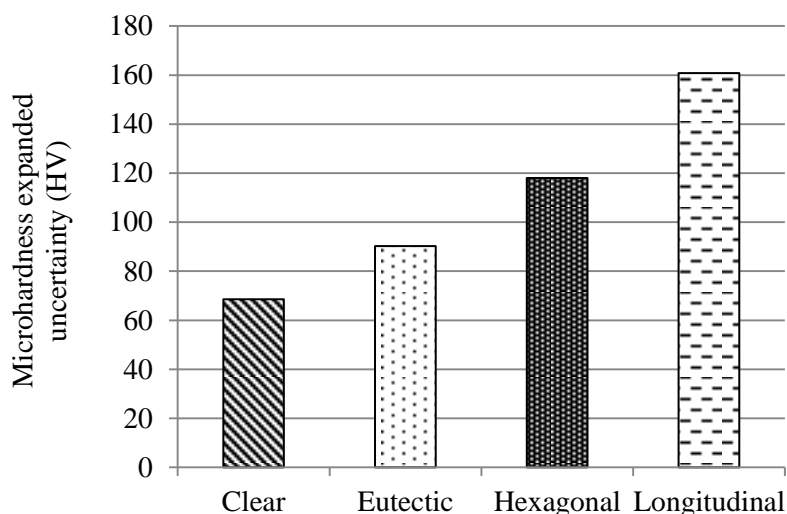


Figure 5. Expanded uncertainty values (95%) associated with the microhardness measurement.

In figure 5, it can be observed that the expanded uncertainty associated with the microhardness assume values of 68 HV, 90 HV, 118 HV and 161 HV for the Clear, Eutectic, Hexagonal and Longitudinal zones, respectively. These figures follow the trend observed for the standard deviation.

The variable that contributed most to the final uncertainty measurement in all cases was the variability of the obtained microhardness values. Note that for the clear zone, the contribution of this variable was 52%, while for the eutectic zone was 50%. In turn, the readings variability was responsible for 46% and 68% of the final uncertainties of the hexagonal and longitudinal zones.

4. Conclusions

The uncertainty of microhardness measurements is highly influenced by the standard deviation of microhardness values, even after applying Chauvenet criterion for extreme values withdrawal.

The presence of M_7C_3 type carbides in a eutectic matrix (carbides + austenite) are indicators of good resistance to abrasive wear of the knives used in sugar mills. The presence of austenite becomes softer the matrix, preventing the release of the carbides.

Acknowledgments

The authors are grateful to FAPEMIG, CNPq and CAPES for financial support.

References

- [1] Dulón J 2003 *Manual de Soldadura para la Industria Azucarera* ed. Talleres de Impresiones gráficas del Ministerio del Azúcar (La Habana) p 116.
- [2] Hugot E 1980 *Manual para Ingenieros Azucareros* Editorial Pueblo y educación (La Habana) p 802.
- [3] SFA 5.13, 2000 Parte C, Section II (AWS A5.13-2000) *Specification for Surfacing Electrodes for Shielded Metal Arc Welding*, pp 305-126.
- [4] Weman K 2003 *Welding process handbook* (New York: CRC Press LLC, ISBN 0-8493-1773-8)
- [5] Ortiz T M et al. 2007 *Electrodo Tubular Revestido para la Reparación de Piezas Sometidas a Desgaste Abrasivo en el Sector Azucarero* (Centro Azúcar, n. 2).
- [6] Procedimiento CIS-MET-030 2002 *Preparación de muestras* Centro de Investigaciones de Soldadura CIS-UCLV.
- [7] Procedimiento CIS-MET-027 2002 *Observación de muestras por microscopia óptica* Centro de Investigaciones de Soldadura CIS-UCLV.

- [8] ASTM E92 2010 Standard Test Method for Vickers Hardness of Metallic Materials.
- [9] EURAMET 2011 Guidelines on the Estimation of Uncertainty in Hardness Measurements EURAMET cg-16 Version 2.0 p 22.
- [10] ISO TAG 4/WG 3 2008 *Guide to the Expression of Uncertainty in Measurement* (Geneva Switzerland) p 141.
- [11] Ellis R A 2003 *Uncertainties of Vickers Hardness Test Blocks* (xvii IMEKO World Congress) June 22 – 27, Dubrovnik, Croatia, pp 982-985.
- [12] Chia-Ming Ch, *et al.* 2010 *Microstructure and wear characteristics of hypereutectic Fe–Cr–C cladding with various carbon contents* Surface & Coatings Technology **205** (doi:10.1016/j.surfcoat.2010.06.021) pp 245–250
- [13] Hsuan-Han L *et al.* 2014 *Effect of Oscillating Traverse Welding on Microstructure Evolution and Characteristic of Hypoeutectic Hardfacing Alloy* Surface & Coatings Technology **239** (<http://dx.doi.org/10.1016/j.surfcoat.2013.11.048>) pp 233–239.
- [14] Buchanan V E, Shipway P H and McCartney D G 2007 *Microstructure and Abrasive Wear Behaviour of Shielded Metal Arc Welding Hardfacings Used in The Sugarcane Industry* Wear **263** (doi:10.1016/j.Wear.12.053) pp 99–110.
- [15] Buchanan V E, McCartney D G and Shipway P H 2008 *A Comparison of The Abrasive Wear Behaviour of Iron-Chromium Based Hardfaced Coatings Deposited by SMAW and Electric Arc Spraying* Wear **264** (doi:10.1016/j.wear.2007.04.008) pp 542–549.
- [16] Stevenson A N J and Hutchings I M 1995 *Wear of Hardfacing White Cast Irons by Solid Particle Erosion* Wear pp186-187, pp 150-158.
- [17] Podchibiakin D *et al.* 2003 *Comparación de Diferentes Métodos de Medición de la Impronta de la Imagen de Microdurómetros* (Jornadas Sam/Conamet/Simposio Materia) pp 1979-82.
- [18] Gabauer W 2000 S M & T Standards Measurement & Testing Project No. SMT4-CT97-2165 *Manual of Codes of Practice for the Determination of Uncertainties in Mechanical Tests on Metallic Materials*, Code of Practice No. 14, The Estimation of Uncertainties in Hardness Measurements, p 16.